Transport and optics in quasi-one-dimensional organic conductors

Leonardo Degiorgi, Denis Jérome

TRANSPORT AND OPTICS IN QUASI-ONE-DIMENSIONAL ORGANIC CONDUCTORS

Leonardo Degiorgi

Laboratorium für Festkörperphysik, ETH Zürich, CH-8093 Zürich, Switzerland

Denis Jérome

Laboratoire de Physique des Solides, UMR 8502,

Université Paris-Sud, F-91405 Orsay, France

Abstract

We review the transport and optical properties of an extended series of low dimensional organic Bechgaard conductors, which are hosting the first organic superconductor $(TMTSF)_2PF_6$. It is shown that all compounds of this family are one-dimensional Mott insulators with an activation energy for longitudinal transport depending on their chemical composition and decreasing under pressure. This activation energy in the transport results vanishes at a (chemical) pressure induced dimensionality cross-over, while a gap feature is still observable in the far-infrared spectrum. Particularly, according to the data of transverse transport, the signature of a gap in the quasi particle spectrum is observable even when the longitudinal transport becomes metal-like. In this survey, we address a variety of relevant problems and concepts associated with the physics of an interacting electron gas in low dimensions, such as non-Fermi liquid behavior, dimensionality crossover, and specifically the appearance of the Luttinger liquid state.

PACS numbers:

INTRODUCTION

The development of science (both physics and chemistry) over the last quarter of the twentieth century has been such that the discovery of superconductivity in organic matter has been achieved in a very particular compound which first shows typical features of low dimensional (namely one dimensional -1D) conductors and second is a member of a much larger family. This vast family is the so-called $(TM)_2X$ series or the Fabre and Bechgaard (FB) series, according to the chemists who discovered the first sulfur TMTTF and selenium TMTSF molecular based compounds, respectively. X denotes an inorganic anion with various possible symmetries, spherical (PF_6, AsF_6, SbF_6, TaF_6), tetrahedral (BF_4, ClO_4, ReO_4) or triangular (NO_3) [1]. The anion in these salts can also be an atom as in the compound $(TMTTF)_2Br$.

All these compounds except the salt of TMTSF with X= ClO_4 do reveal an insulating ground state for reasons that may actually differ between compounds. For instance, the mechanism driving the metal-insulator transition at 12 K in $(TMTSF)_2PF_6$ at ambient pressure is the onset of itinerant antiferromagnetism that induces magnetic modulation, called the spin density wave (SDW). Although SDW formation has been proposed earlier for the interpretation of the magnetic transition in chromium, due to the nested regions of the peculiar Fermi surface of this 3-D metal [2, 3], it has particularly dramatic consequences in the case of the quasi planar Fermi surfaces of Bechgaard salts. With a band filled up to the wave vectors $\pm k_F$, the exchange term of the Hartree-Fock potential, which is also characterized by the same wave vector $2k_F$, opens a gap at the Fermi level over the entire surface giving rise to an insulating ground state. However, as far as the sulfur analog $(TMTTF)_2PF_6$ is concerned, its insulating character is a result of the Coulomb repulsion between 1D electrons, as will be discussed below.

Shortly after the discovery of superconductivity in $(TMTSF)_2PF_6$, [4] many other members of the same series with a variety of anions have also been found to exhibit superconductivity at temperatures close to 1 K at a high pressure in a 10 kbar domain [5]. Nevertheless, $(TMTSF)_2ClO_4$ is the only member of the $(TMTSF)_2X$ series that has so far exhibited superconductivity at low temperatures under atmospheric pressure [6]. Hence, a unified $(TM)_2X$ phase diagram has been proposed experimentally (Fig. 1) [7]. This diagram suggests that very different systems such as the

superconducting $(TMTSF)_2ClO_4$ and the strongly insulating $(TMTTF)_2PF_6$ belong to the same class of materials, *i.e.*, the physical properties of the latter can be made equivalent to those of the former provided that a sufficiently high pressure is applied.

First, it is instructive to look at the band structure that can be expected of these materials on the basis of a single particle model using a tight binding (TB) scheme and a few simplifications. One is the use of the highest occupied molecular orbital (HOMO) as the starting wave function for the TB calculation which is justified by the only weak interaction existing between molecules in the solid state. The other is the extended Hückel method, which leads to an appropriate band description. The band structure parameters thus obtained can be used to define the following model of the energy spectrum [8, 9]:

$$\epsilon(\vec{k}) = -2t_a \cos(k_a a/2) - 2t_{\perp b} \cos(k_{\perp b} b) - 2t_{\perp c} \cos(k_{\perp c} c), \tag{1}$$

with an orthorhombic approximation to the actual triclinic structure. The conduction band along the chain direction has an overall width $4t_a$ ranging between 0.4 and 1.2 eV, depending on the chemical nature of the donor molecule. Since the overlap between electron clouds of neighboring molecules along the stacking direction is about 10 times larger than that between the stacks in the transverse b direction and 500 times larger than that along the c direction, the electronic structure can be viewed at first sight as one-dimensional with an open and slightly warped Fermi surface centered at the Fermi wave vector $\pm k_F$ defined for isolated chains.

Anions located in centrosymmetrical cavities lie slightly above or below each molecular plane. This structure results in the dimerization of the intermolecular distance (overlap) with a concomitant splitting of the HOMO conduction band into a filled lower band separated from a half-filled upper (hole-like) band by a gap Δ_D at $\pm 2k_F$, called the dimerization gap in the new Brillouin zone. However, on account of the finite transverse dispersion, this dimerization gap does not lead to a genuine gap in the middle of the density of states as shown from the extended-Hückel band calculation. The only claim that can be made is that these conductors show commensurate band filling (three quarter filled with electrons or one quarter empty with holes). This originates from the 2:1 stoichiometry with a tendency towards half filling which is more pronounced for sulfur (with enhanced structural dimerization) than for selenium compounds. Consequently, according to single particle band calculation, all compounds in the $(TM)_2X$ series should exhibit conductivity.

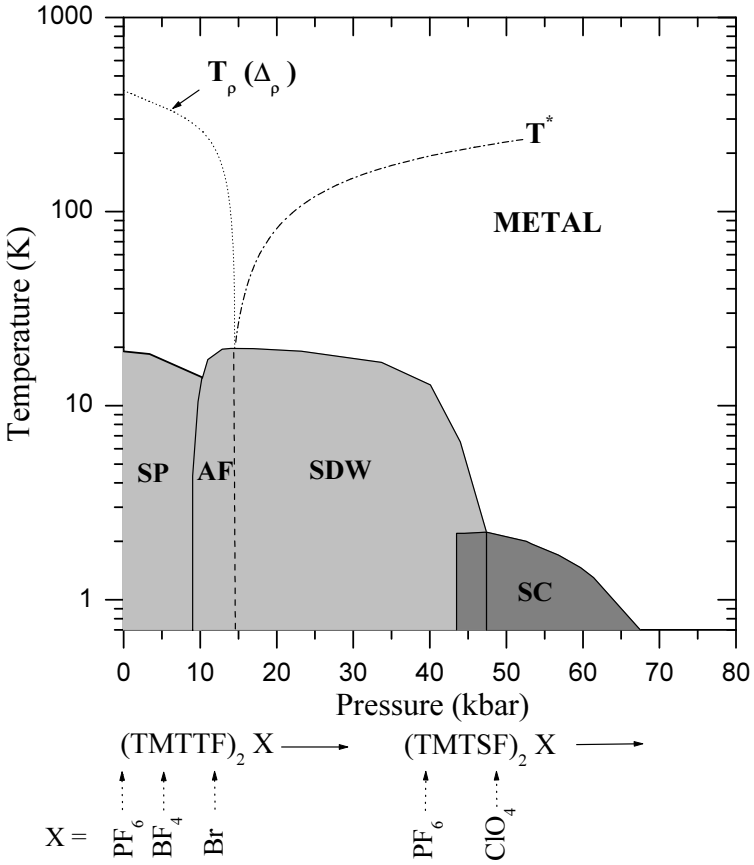

Figure 1: Generic phase diagram for $(TM)_2X$ compounds based on $(TMTTF)_2PF_6$ as pressure origin [7]. SP denotes spin-Peierls, AF antiferromagnetic, SDW spin-density-wave and SC superconducting.

In Table (I) we report the band parameters of different members of the $(TM)_2X$ series as computed from crystallographic data [10]. The sulfur compounds exhibit bands that are significantly narrower and their crystallographic structure is more dimerized than those of the selenide compounds. $(TMTTF)_2Br$ (not listed in Table (I)) is however an exception among the sulfur compounds with a dimerization of 0.13 which is smaller than the value calculated for $(TMTSF)_2ClO_4$. This might be due to the calculation of electronic bands based on rather old and less accurate crystallographic data than those used for the other compounds [11].

The gross features of the $(TM)_2X$ phase diagram are shown in Fig. 1. Compounds on the left hand side of the phase diagram, such as $(TMTTF)_2PF_6$, are insulators below room temperature with a broad metal to insulator transition, while those on the right hand side of $(TMTTF)_2Br$ exhibit an extended temperature (T) regime with a metallic behavior and

	$(TMTTF)_2PF_6$	$(TMTSF)_2PF_6$	$(TMTSF)_2ClO_4$
t_1	137	252	258
t_2	93	209	221
$\bar{t}$	115	230	239
$\frac{\Delta t}{\bar{t}}$	0.38	0.187	0.155
$\overline{t_\perp}$	13	58	44

Table I: Calculated band parameters for three representative members of the $(TM)_2X$ series according to the room temperature crystallographic data in reference [10]. The average intra and interstack interactions are given in lines 3 and 5 respectively. The bond dimerization is shown in line 4. All energies are in meV.

a sharp transition towards an insulating ground state. Therefore, the cause of the insulating nature of some members of the $(TM)_2X$ series should be determined in relation to the role of e-e repulsion and low dimensionality as we shall show later. Although the most extensive pressure studies have been performed on $(TMTSF)_2PF_6$ and $(TMTTF)_2PF_6$, recent studies of other compounds of the $(TMTTF)_2X$ series with X= ReO_4, BF_4 and Br have shown that the main features observed in $(TMTTF)_2PF_6$ or in $(TMTSF)_2PF_6$ under pressure are also observed in other systems [12].

In addition, organic chemistry has provided us with quite complementary compounds, such as $(EDT-TTF-CONMe_2)_2AsF_6$[13] and $(TTDM-TTF)_2Au(mnt)_2$[14], which, although exhibiting a stacking of the organic cations similarly to that in the case of $(TM)_2X$ materials, differ from them in chemistry or the location of the anions in the structure. These compounds have contributed to disentangle the intricate properties of the 1D $(TM)_2X$ compounds.

TRANSPORT PROPERTIES

Although the $(TM)_2X$ generic phase diagram can be established by measuring the transport properties of various compounds, it is most rewarding to use a single compound, namely $(TMTTF)_2PF_6$, and the help of a high pressure. The study of this strongly insulating system $(TMTTF)_2PF_6$ at a high pressure has been very useful not only because it has led to

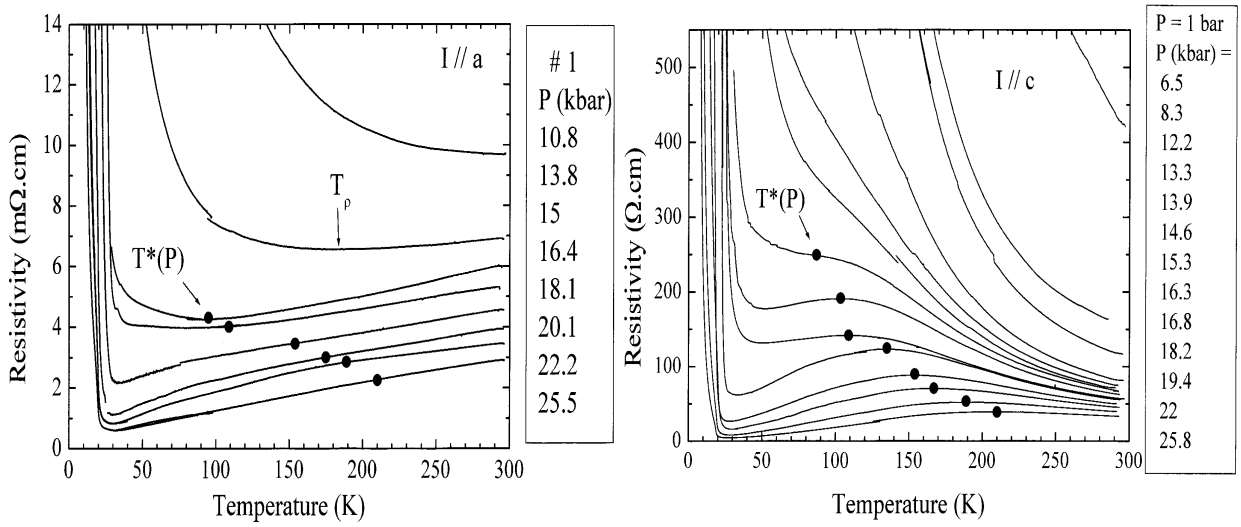

Figure 2: $(TMTTF)_2PF_6$ longitudinal (left) and transverse (right) resistances versus temperature at different pressures [12].

the stabilization of superconductivity in a strongly insulating sulfur compound [15] but also because its location at the left end of the phase diagram has allowed several key properties of quasi 1-D conductors to be carefully monitored under pressure, for instance, the longitudinal or transverse transports and the one dimensional deconfinement arising under pressure [12]. The phase diagram in Fig. 1 where $(TMTTF)_2PF_6$ is the reference compound at ambient pressure has been obtained from the temperature dependences of $\rho_c(T)$ and $\rho_a(T)$ to be discussed below. In the low pressure region (see Fig. 2, P <10 kbar) $\rho_c(T)$ and $\rho_a(T)$ are both activated, with Δ_c being about 30% larger than Δ_a. At higher pressures, the activation of ρ_c follows a gentle decrease, while Δ_a collapses abruptly at a pressure of about 14 kbar, which also marks the onset of a maximum of ρ_c at the temperature $T^\star$ (Fig. 3).

Above 14 kbar, $\rho_a(T)$ displays a metallic temperature dependence down to the sharp metal-insulator transition below 20 K, while $\rho_c(T)$ remains indicative of a weakly insulating state above the temperature $T^\star$ which is increasing under pressure. The insulating character of these materials with partly filled conduction bands is not expected in the framework of non interacting electrons. The reason for this must be the existence of strong repulsive interactions between 1D carriers. The different values and pressure dependences of the activation energies can be taken as evidence of in-chain conduction made possible by thermally excited 1-D objects similar to solitons in conducting polymers [16], whereas transverse transport

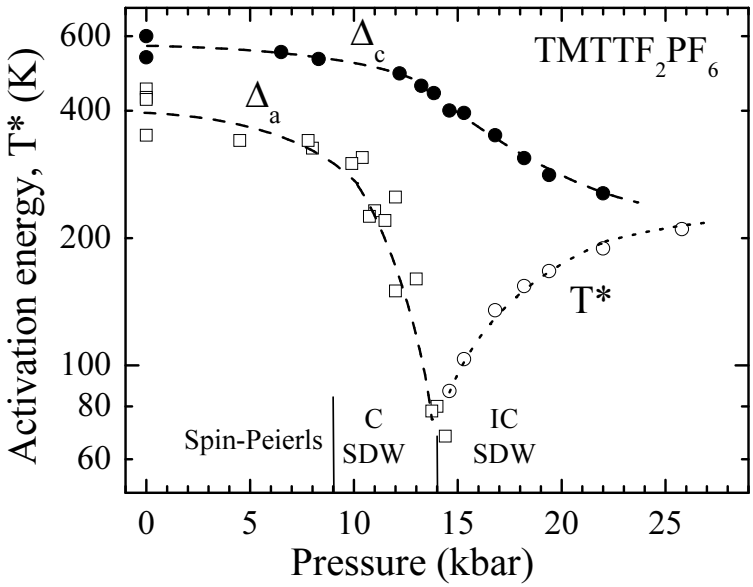

Figure 3: Pressure dependence of transport activation in $(TMTTF)_2PF_6$. The activation for the c axis transport (Δ_c) although decreasing under pressure survives up to high pressures while the longitudinal transport (Δ_a) is no longer activated above 15 kbar when a dimensional cross-over occurs at a finite temperature [12].

requires the excitation of quasiparticles (QPs) through a Mott-Hubbard gap larger than the soliton gap.

What 1-D physics means is that instead of the usual description of low-lying excitations in terms of QP states in the Landau-Fermi liquid model, a collective mode description with decoupled spin and charge modes is a more appropriate starting point [17–19]. Such a model for 1D conductors has been proposed on the basis of a linearized energy spectrum for excitations close to the Fermi level and adding the relevant Coulomb repulsions which are responsible for electron scattering with momentum transfer $2k_F$ and 0. This is the popular Tomonaga-Luttinger (TL) model for a 1-D conductor in which the spatial variation of all correlation functions (spin susceptibility at $2k_F$ or $4k_F$, CDW, superconductivity) exhibit a power law decay, characterized by the non-universal exponent K_ρ (which is a function of microscopic coupling constant) [20]. When K_ρ is larger than unity, interactions between carriers become attractive and favor superconducting correlations at a low temperature whereas, if K_ρ is less than unity, repulsive interactions together with magnetic correlations are enhanced at a low temperature [21].

However, there exists an added peculiarity in these 1D conductors. The filling of the conduction band is commensurate. The stoichiometry imposes half a carrier (hole) per TM molecule, a concentration that cannot be modified by applying pressure. Consequently, uniformly spaced molecules along the stacking axis should lead to a situation where a unit cell contains 1/2 carriers, *i.e.*, the conduction band is quarter-filled. However, the non-uniformity of molecular packing has been observed in early structural studies of the $(TMTTF)_2X$ crystals [10]. The dimerization of the overlap between molecules occurs along the stacks, a situation which is pronounced in the sulfur series, although it is also encountered in some members of the $(TMTSF)_2X$ series (Table 1). The impact of such dimerization on the electronic structure is generally quantified by modulating of the intra-stack overlap integral because both longitudinal and transverse molecular displacements can contribute to the modulation of the intermolecular overlap and could make them half-filled band compounds. Commensurate band filling opens a scattering channel for the carriers between both sides of the Fermi surface so that the total momentum transfer for two (four) electrons from one side of the 1D Fermi surface to the other is equal to a reciprocal lattice vector (Umklapp scattering for half (quarter)-filled bands)[21]. Commensurability leads to important modifications in the model of the gapless Luttinger liquid, driving it towards a Mott-Hubbard type insulator with a gap in the charge sector; however, on account of the spin-charge separation of the 1D physics the spin sector remains gap-less [21]. The amplitude of the charge gap very strongly depends on band filling and the strength of the e-e repulsions of the 1D electronic spectrum. For half-filled band 1D conductors the Mott Hubbard gap opens up as soon as the interactions between carriers become infinitesimally repulsive namely, $K_\rho < 1$. Quarter-filled band conductors however require more repulsive interactions before becoming 1D insulators. They become insulating when the condition $K_\rho < 0.25$ is fulfilled.

The gap for conduction along the chains thus reads [21]

$$2\Delta_a \approx W(\frac{g_U}{W})^{1/(2-2\tilde{n}^2 K_\rho)}, \tag{2}$$

where g_U is the coupling constant $g_U = W(\frac{U}{W})^3$ and $\tilde{n} = 2$ (1) for the 1/4 (1/2)-filled situation in the Hubbard limit. Although the insulating behavior of $(TM)_2X$ salts can be clearly ascribed to their commensurate band filling a closer examination is needed to determine which of the Umklapp scattering channels 1/2 or 1/4 filled is the most active. In the presence of such a gap, the transport is activated at low temperature $\rho_\parallel \approx e^{\Delta_a/T}$ but is

expected to vary according to the power law

$$\rho_{\parallel} \approx T^{4\tilde{n}^2 K_\rho - 3} \tag{3}$$

in the high temperature regime, *i.e.*, $T > \Delta_a$ [21]. The material resembles a metal at high temperature along the longitudinal direction. In the high T regime ($T > t_\perp$), the picture of non-coupled chains is approached. Therefore, the density of quasiparticle states should resemble the situation that prevails in a Luttinger liquid namely, $N(E) \approx \mid \omega \mid^{\alpha}$, where α is related to K_ρ through $\alpha = \frac{1}{4}(K_\rho + 1/K_\rho - 2)$, forgetting about the influence of the Mott gap (supposedly smaller than the temperature).

From early measurements in $(TMTSF)_2PF_6$ at ambient pressure opposite temperature dependences for ρ_a and ρ_c has been reported in the high temperature regime [22]. This phenomenon has been revisited later including a high pressure study in $(TMTSF)_2PF_6$ and $(TMTTF)_2PF_6$ [23] and recently in an extensive high pressure investigation of several $(TM)_2X$ compounds [24] (Fig. 4).

The behavior of the $(TMTSF)_2PF_6$ resistance along the direction of the weakest coupling, *i.e.*, along the c-axis, displays an insulating character with a maximum around 80-100 K and becomes metallic at lower temperatures, although remaining several orders of magnitude above the Mott-Ioffe critical value which is considered as the limit between metal and insulating-like transport [25].

The insulating character of the transverse transport has been interpreted as the signature of a non Fermi-Landau behavior for carriers within planes (chains) [23]. When transverse transport along the c-direction is incoherent, transverse conductivity probes the physics of the $a-b$ planes and conductivity in terms of the transverse coupling $t_\perp$ is expressed in tunneling approximation as

$$\sigma_\perp(\omega, T) \alpha t_\perp^2 \int dx \int d\omega' A_{1D}(x, \omega') A_{1D}(x, \omega + \omega') \times \frac{f(\omega') - f(\omega' + \omega)}{\omega}, \tag{4}$$

where $A_{1D}(x, \omega)$ is the one-electron spectral function of a single chain and $f(\omega)$ the Fermi-Dirac function. When the $a-b$ plane is an array of weakly interacting Luttinger chains, eq. (4) leads to a power law temperature dependence for the c-axis conduction. The temperature at which the c-axis transport switches from an insulating to a metallic temperature

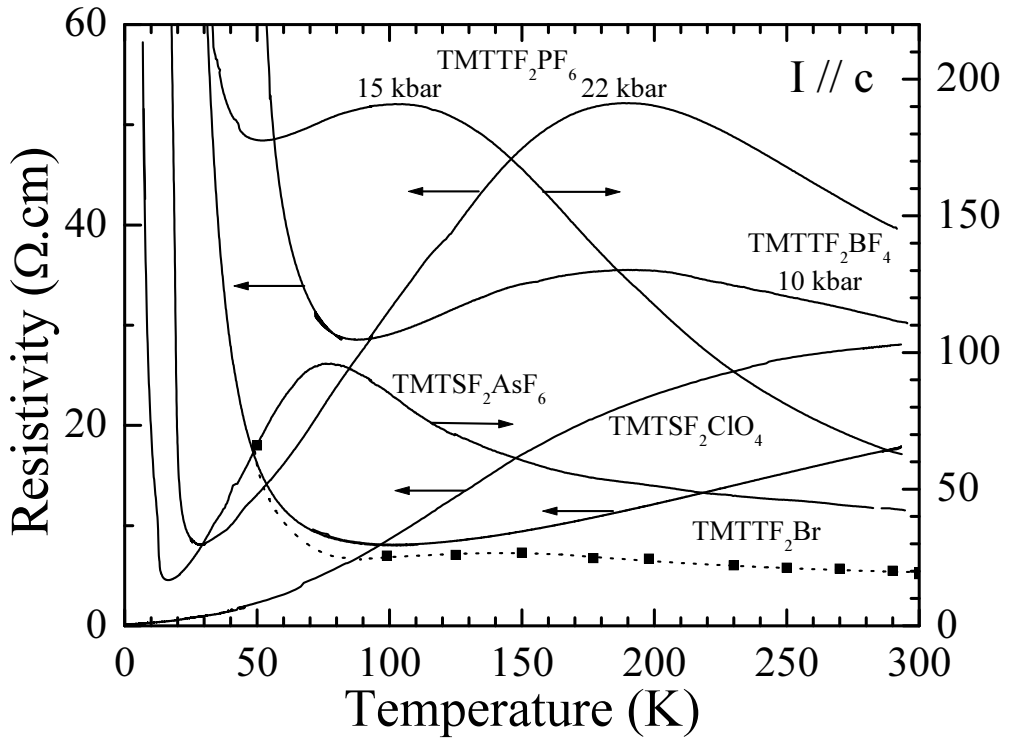

Figure 4: Temperature dependence of the transverse transport along the c-axis in several compounds belonging to the $(TM)_2X$ series studied under pressure. The temperature of the maximum of resistivity shows the location of the dimensional cross-over which is strongly pressure dependent for each compound. The resistivity minimum at low temperatures represents the stabilisation of the insulating SDW phase. In case of the selenium compound $TMTSF_2ClO_4$ the cross-over lies around room temperature whereas for the sulfur compound $TMTTF_2Br$ a resistivity maximum is seen only after the constant volume correction is taken into account [24].

dependence corresponds to a cross-over between two regimes; a high temperature regime with no QP weight at the Fermi energy (possibly a TL liquid in the 1D case) and another regime in which the QP weight increases with decreasing temperature. This interpretation does not necessarily imply that the transport along the c-direction must also become coherent below the cross-over. The c-axis transport may well remain incoherent with a Fermi liquid being established in the $a-b$ plane at temperatures below $T^\star$. The resistivity along the least conducting direction is thus expressed as [26]:

$$\rho_c(T) \approx T^{1-2\alpha}. \tag{5}$$

Consequently, the temperature dependence of transport properties along the a and c-axes

above $T^\star$ should possibly lead to a consistent determination of K_ρ.

A major problem encountered with the $(TM)_2X$ materials (and also in most organic conductors) is the very strong pressure (or volume) dependence of their electronic properties, particularly the transport property [27–29]. In addition, the thermal expansion of these materials is particularly large. Hence, the only temperature dependence that can be compared with the prediction of the theory is the one measured at a constant volume. As all temperature dependences are obtained at a constant pressure, a transformation at a constant volume has to be performed. An example is given in Fig. 5 by the longitudinal

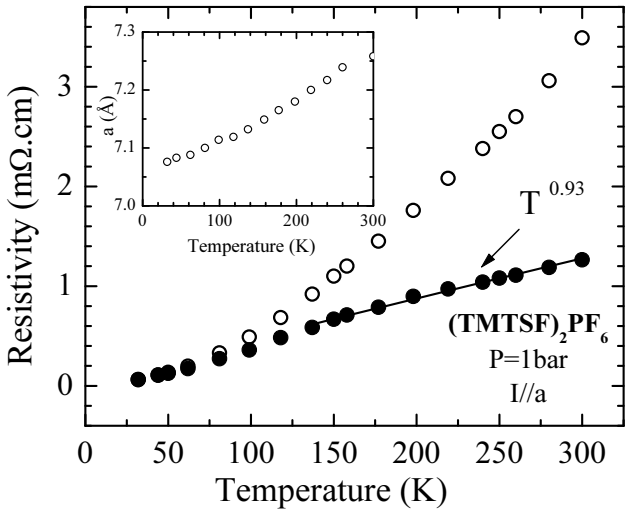

Figure 5: Temperature dependence of the $(TMTSF)_2PF_6$ longitudinal resistance at constant volume showing quasi linear T-dependence, with the thermal dependence of the lattice parameter a displayed in the inset [29].

transport of $(TMTSF)_2PF_6$ behaving at a high temperature similar to T^2 under ambient pressure but varying sublinearly ($\approx T^{0.93}$) from 300 to 150 K once volume correction is taken into account [29]. The experimental power law of longitudinal resistivity leads in turn to $\tilde{n}^2 K_\rho$=0.98 according to the theory of resistivity. Note that a similar power law for the temperature dependence of longitudinal transport ($\approx T^{0.93}$) can also be observed for two other sulfur-compounds, BF_4 and PF_6under pressure when the correction to constant volume becomes negligible.

In the early days of the $(TM)_2X$ compounds the lattice dimerization was believed to govern the amplitude of the Mott-Hubbard gap [30, 31]. If we choose the half filled hypothesis ($\tilde{n} = 1$), given as $\tilde{n}^2 K_\rho$=0.98, then K_ρ is close to unity implying a weakly coupled electron

gas. This situation of a very weak coupling is difficult to reconcile with an enhancement of the spin susceptibility [19] but an additional argument against this weak coupling is made possible by the unusual behavior of transverse transport (eq. (5)) [26]. The weak coupling value for $K_\rho \approx 1$ derived from the temperature dependence of longitudinal transport and the optical data (see below) would imply $\alpha \approx 0$ and consequently a metal-like temperature dependence for $\rho_c(T)$ which is *at variance* with the data.

More recently, an alternative interpretation based on new experimental results has been proposed assuming that the 1/4-filled scattering could justify the existence of the Mott gap in the entire $(TM)_2X$ series [21]. With such a hypothesis ($\tilde{n} = 2$), the fit of the experimental data would thus lead to $K_\rho = 0.23$ and $\alpha = 0.64$ (see below, discussion on optical response) [32]. This value for K_ρ agrees fairly well in the 1/4 filled scenario with band structure calculations and plasma edge measurements and $U/W = 0.7$ (which is in fair agreement with an increase in spin susceptibility at low temperatures) [19]. Such a strong coupling value for K_ρ implies that a system such as $(TMTSF)_2PF_6$ lies at the border between a 1D Mott insulator and a Luttinger liquid, though slightly on the insulating side. $(TMTTF)_2Br$ is another particularly interesting system, in which the pressure coefficient of resistivity is very large. Hence, the correction to a constant volume makes the maximum in ρ_c to appear around 150 K while this maximum is absent in constant pressure runs (Fig. 4).

Even if a debate between 1/2 and 1/4 fillings may be relevant for $(TM)_2X$, this is no longer the case for new synthesized compounds in a family whose general structure precludes any dimerization. The structural peculiarity of the salt $(EDT-TTF-CONMe_2)_2AsF_6$ is the absence of inversion center between adjacent molecules in stacks and instead the presence of a glide plane symmetry [13]. The analysis of the transport data of $(EDT-TTF-CONMe_2)_2AsF_6$ has shown that in spite of the existence of a glide plane symmetry the carriers are localized, and even more localized than in the most insulating salts of the Fabre series known at present. Since the localization in this compound cannot be ascribed to a 1/2−Umklapp scattering or to the Anderson localization, 1/4-Umklapp scattering seems to be the only channel left to explain carrier localization in this commensurate 1D conductor. Under ambient pressure, given the total bandwidth deduced from quantum chemistry ($W_0 = W_{tot}(P = 1 \text{ bar}) = 0.350$ eV (3850 K)) and the experimental Mott gap ($2\Delta_a = 2700$ K), the theory [21] gives, in the case of quarter filling *stricto sensu*: $2\Delta_a = W(\frac{U}{W})^{2/(1-4K_\rho)}$. This leads to $K_\rho = 0.1$, with a reasonable $U/W_0 = 0.9$. The Mott

gap of $(EDT-TTF-CONMe_2)_2AsF_6$is much larger than the expected value of the bare interstack overlap $t_\perp$ (which is similar to that value of $(TMTTF)_2Br$, *i.e.*, on the order of 100-200 K and even larger than that observed in the transverse coupling of $(TMTTF)_2PF_6$). Consequently, the large Mott gap makes the single particle hopping between neighboring stacks irrelevant, at least, in the pressure regime less than 20 kbar since the transverse hopping is renormalized to zero on account of a relevant intrachain electron-hole interaction.

A U/W_0 such as 0.9 is in fair agreement with the result of a crude analysis of the spin susceptibility of S-salts [19] and indicates that these compounds lie in the strong coupling limit. With increasing pressure, the gap decreases steadily up to the pressure of 20 kbar above which it disappears sharply due to the competing transverse coupling. Below 15 kbar, the gap of $(EDT-TTF-CONMe_2)_2AsF_6$(1350 K) is about equal to the gap of $(TMTTF)_2X$ measured under ambient pressure [23]. Since the logarithmic pressure dependences of the gap seem to be similar for both compounds, we may say that $(EDT-TTF-CONMe_2)_2AsF_6$can also be considered as part of the same FB salt diagram, provided that the origin of the pressure axis is shifted to the left by 15 kbar. Hence, it is reasonable to expect that the TL parameter K_ρ increases from left to right in the $(TM)_2X$ diagram, since both optical and transport data suggest K_ρ= 0.23 in the Se compounds.

Now, regarding $(TMTTF)_2PF_6$, we are facing a very interesting system, since the evolution from a Mott insulator to a metal can be carefully studied under pressure in a single sample and a decrease in compressibility under pressure makes constant volume correction less significant for temperature dependences measured at high pressures. Turning to the evaluation of the correlation coefficient from the temperature dependence of ρ_c we end up fitting the data for $(TMTTF)_2PF_6$ in the pressure domain around 12 kbar, Fig. 2, with a very small value of K_ρ (or large values of α) which is not compatible with the value $K_\rho = 0.23$ derived from the far infrared (FIR, see below) and NMR data [19]. Consequently, the Mott gap seems to be important in this temperature regime governing the excitation for the motion of single particles along c. Tentatively, one can expect a transverse resistivity behaving according to [26],

$$\rho_c(T)\alpha T^{1-2\alpha}\exp\Delta_c/T. \tag{6}$$

Since the Mott -Hubbard gap varies exponentially with K_ρ even a small variation in the ratio between the Coulomb interaction and the bandwidth under pressure can explain a significant

decrease of all gaps moving from the left to the right in the generic phase diagram. Both optical (see below) and transport data give $2\Delta_a = 800-1000$ K in $(TMTTF)_2PF_6$ at ambient pressure [12]. The difference between K_ρ for selenium and sulfur compounds ($K_\rho = 0.18$ for the latter material) is a result of the difference between their bare bandwidths, since on-site repulsion, being a molecular property, is likely to be less sensitive to pressure than the intermolecular overlap along the stacking axis.

The dominant role of the intra-stacks overlap in the pressure dependence of the Mott gap on the left hand side of the diagram is corroborated by the behavior of the very one-dimensional compound $(TTDM-TTF)_2Au(mnt)_2$which remains robustly insulating up to 25 kbar at least [14]. The peculiar arrangement of the anions in this compound with their molecular planes perpendicular to the donor stacks provides in turn a very high 1D confinement. This particular structure enables us to differentiate between the role of pressure on the bandwidth and the transverse coupling suppressing the 1D character. It has been shown recently by a dynamic mean field approach [33] that the Mott localization, a purely one dimensional effect, is severely suppressed by the onset of transverse coupling. Crudely speaking, the localization vanishes when the transverse coupling and the 1D Mott gap are of the same order of magnitude.

The lesson is that the members on the left-hand side of the phase diagram $(TM)_2X$ are indeed 1D confined Mott insulators with a correlation gap for longitudinal transport evolving first slowly under pressure due to the pressure-induced band broadening and then collapsing due to the growth of the inter-stack coupling. $(TMTSF)_2PF_6$ under ambient pressure looks like a 1D metal at high temperatures because the temperature is large compared to the Mott gap. This compound remains a metal below the cross-over temperature $T^\star$ seen on ρ_c and the one dimensional carriers are deconfined by a transverse coupling which is then larger than the Mott gap [21]. We now wish to support this view and scenario from the perspective of the electrodynamic response.

OPTICAL PROPERTIES

Spectroscopic techniques are generally useful for shedding light on microscopic electronic properties. Optical studies, in particular, give a rather thorough insight into ground-state

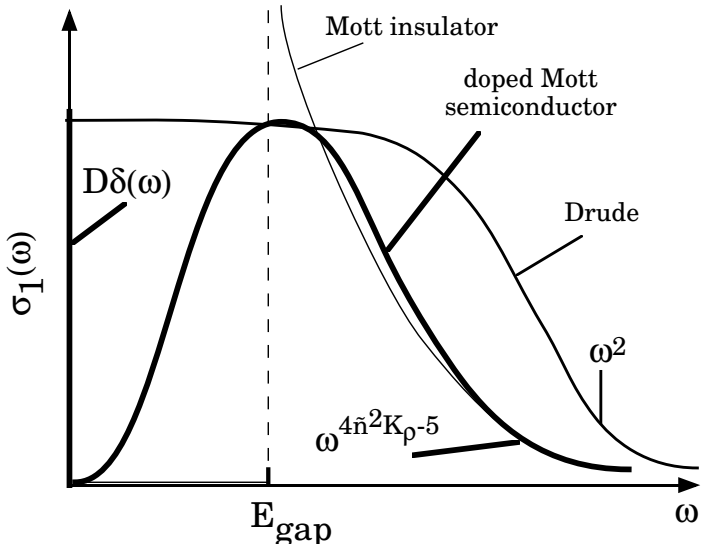

Figure 6: Optical conductivity of the Mott insulator and of the doped Mott semiconductor [21, 35]. The simple Drude behavior is shown for comparison.

properties and reveal the unusual nature of correlations in 1D [34]. Moreover, the optical properties collected at different polarizations of light allow disentangling the physics for anisotropic materials. From a theoretical point of view for a strict one-dimensional Mott insulator (i.e., zero transverse coupling), the charge correlation gap E_{gap}, corresponding to the excitation between the lower and upper Hubbard bands, appears as a standard square-root singularity in the charge excitation spectrum (i.e., in the real part $\sigma_1(\omega)$ of the optical conductivity, Fig. 6) [21, 35]. This is the situation predicted by the 1D TL liquid model, when taking into account the so called Umklapp scattering process. The scenario calculated for a doped one-dimensional Mott semiconductor, on the other hand, consists of a Mott gap (as reminder of the original 1D limit with Umklapp scattering process) and a zero-energy mode (i.e., theoretically a $D\delta(\omega)$ function at $\omega = 0$, representing the Drude resonance of the effective metallic contribution with scattering rate $\Gamma = 0$) for low doping levels (Fig. 6) [21, 35]. The spectral weight D encountered in the "Drude resonance" is proportional to the effective charge doping level, induced by the transverse interchain coupling $t_\perp$, in the

upper Hubbard band. Of course for the low-energy mode, this is an oversimplified view, since the interchain hopping makes the system two dimensional, and the low-energy feature is unlikely to be described by a simple one-dimensional theory [21, 35]. Because of the zero energy mode and the finite dc conductivity, the transition across the charge correlation gap is now a pseudogap excitation. Therefore, due to the deviation from the strict one-dimensional limit, such an excitation is no longer a singularity at E_{gap} but rather a broad feature (Fig. 6). $t_\perp$ becomes ineffective at sufficiently high temperatures or frequencies. Consequently for $T, \omega \gg t_\perp$ and $T, \omega \gg E_{gap}$ we expect the 1D physics (i.e., the Mott insulating state) to be dominant. At such high energies for both ω and T, the warping of the Fermi surface, induced by $t_\perp$, is neither relevant nor observable. The theory predicts a powerlaw behavior $\sigma_1(\omega) \sim \omega^{-\gamma}$ (Fig. 6) [21, 35, 36]. The exponent γ is characteristic of the correlations dominating in the system.

By combining the results obtained using different spectrometers in the microwave, millimeter, submillimeter, infrared, visible and ultraviolet ranges, we have achieved the electrodynamic response over an extremely broad energy range (10^{-5}-10 eV) for the compositions $(TMTSF)_2X$ and $(TMTTF)_2X$, where X is a counterion such as Br, ReO_4, ClO_4, PF_6 and AsF_6 [35, 37–39]. Figure 7 shows the temperature dependence of the real part $\sigma_1(\omega)$ of the optical conductivity in different Bechgaard salts for $E \| a$, the chain direction. Part (a) shows $\sigma_1(\omega)$ for the Br compounds of the TMTTF family, while part (b) displays $\sigma_1(\omega)$ for $(TMTSF)_2PF_6$. We can immediately remark that the temperature dependence of $\sigma_1(\omega)$ is quite important for all compounds.

The optical conductivities of the TMTTF salts display several absorption features, mainly due to the inter and intramolecular vibrations of the TMTTF unit. These vibrations can even be enhanced by the electron-phonon coupling [35]. The phonon modes are particularly observed in the TMTTF salts, because the screening by free electrons is less effective owing to the insulating state at low temperatures. The identification of the charge gap (E_{gap}), based on the optical spectra, is not straightforward, because of the large phonon activity. Thus, the results of other measurements were used. The gap values obtained for $(TMTTF)_2X$ with different techniques are displayed in Fig. 7a. The low-temperature dielectric constant (ϵ) measured at 100 GHz is consistent with E_{gap}= 50 meV for $(TMTTF)_2Br$, while the photoemission spectra suggest a E_{gap}= 60 meV [35, 38]. Therefore, the absorptions in $\sigma_1(\omega)$ near 35 meV for $(TMTTF)_2Br$ and at 99 meV for $(TMTTF)_2PF_6$ (not shown) are associated

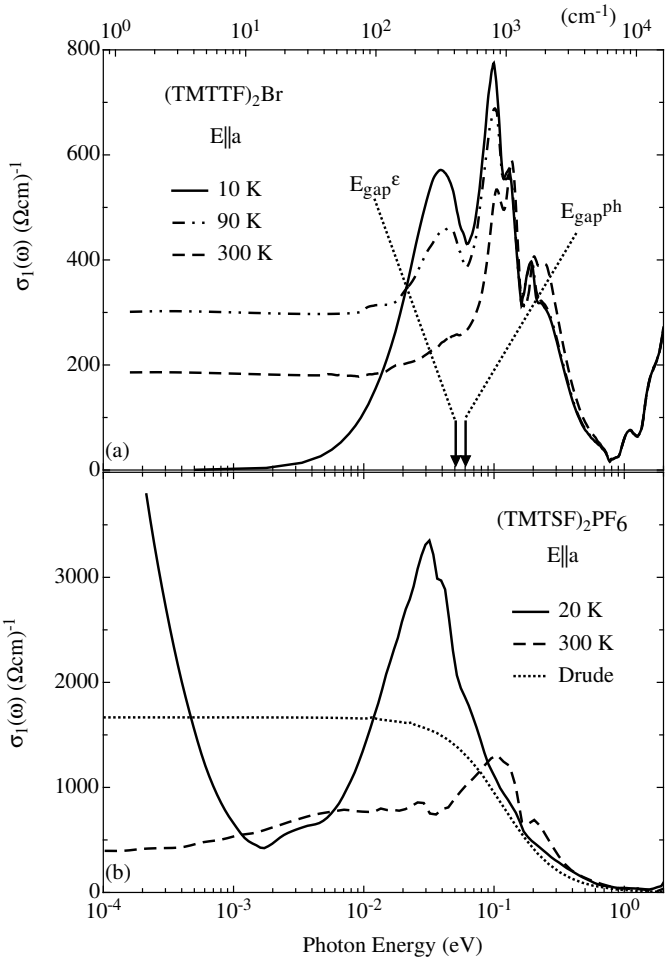

Figure 7: On chain optical conductivities of (a) $(TMTTF)_2Br$ and (b) $(TMTSF)_2PF_6$ at temperatures above the transitions to the broken symmetry ground states. The arrows indicate the gaps observed by dielectric (ϵ) response and photoemission (ph) experiments. A simple Drude component is also shown in panel (b). Note that photoemission measures the quantity $E_{gap}/2$, assuming that the Fermi level is in the middle of the gap [35, 37–39].

with E_{gap}.

The optical properties of the $(TMTSF)_2X$ analogs (Fig. 7b), for which the dc conductivity gives evidence of metallic behavior down to low temperatures (just above the SDW phase transition), are markedly different from that of a simple metal. A well-defined absorption feature around 25 meV (later ascribed to the correlation pseudogap) and a zero-frequency mode are observed at low temperatures [35, 37, 38]. The latter mode at low temperatures is narrower in $(TMTSF)_2ClO_4$ (not shown here) than in $(TMTSF)_2PF_6$.

In both cases, due to full charge transfer from the organic molecules to the counterions and depending on the importance of the dimerization, the band of the TMTTF or TMTSF stacks can be described as either half-filled (for a strong dimerization effect) or quarter-filled (for a weak dimerization effect). As pointed out before, because of the commensurate filling, a strictly one-dimensional TL liquid with Umklapp scattering effects is unstable and transforms into a Mott insulating state, which is dominated by the charge correlation gap excitation (Fig. 6). Indeed, the $(TMTTF)_2X$ salts, with X=PF_6 or Br, are insulators at low temperatures [8] with a substantial (Mott) charge gap. For these compounds the correlation gap E_{gap} is so large that the interchain hopping ($t_\perp$) is not relevant. Charge carrier hopping on parallel chains is here strongly suppressed leading to a truly 1D insulating phase [21]. In analogy to the TMTTF salts, the strong FIR excitation of the TMTSF salts is ascribed to the so-called pseudo charge correlation gap. The existence of a gap feature in the metallic state, containing nearly all of the spectral weight, is at first sight similar to what is expected for a band-crossing transition for simple semiconductors, which would result in a semimetallic state.

The nearly temperature-independent magnetic susceptibility, which gives strong evidence of a gapless spin excitation spectrum (this has often been interpreted as a Pauli susceptibility or as the susceptibility due to a large exchange interaction), demonstrates that the state is not a simple semimetal. The existence of a gap, or pseudogap in the charge excitations with the absence of a gap for spin excitations, indicates spin-charge separation in the metallic state. This spin-charge separation is, however, distinct from that of a 1D TL liquid, in which both excitations are gapless but have different dispersion velocities. Here, it is the Umklapp scattering, which leads to gapped charge excitations.

The narrow zero-energy mode seen in the spectra of the TMTSF family at low frequencies is the experimental optical fingerprint of the theoretically predicted Drude peak for the quasi two-dimensional Mott semiconductor [21]. Such a peak contains only 1% of the carriers (i.e., 1% of the total spectral weight). Although no real doping exists from a chemistry point of view, the narrow Drude peak originates from deviations of commensurability due to the interchain coupling ($t_\perp$). If $t_\perp(\sim t_b)$ between chains is relevant (i.e., $t_\perp > E_{gap}$), small deviations from commensurate filling due to the warping of the Fermi surface exist, and should lead to effects equivalent to real doping on a single chain.

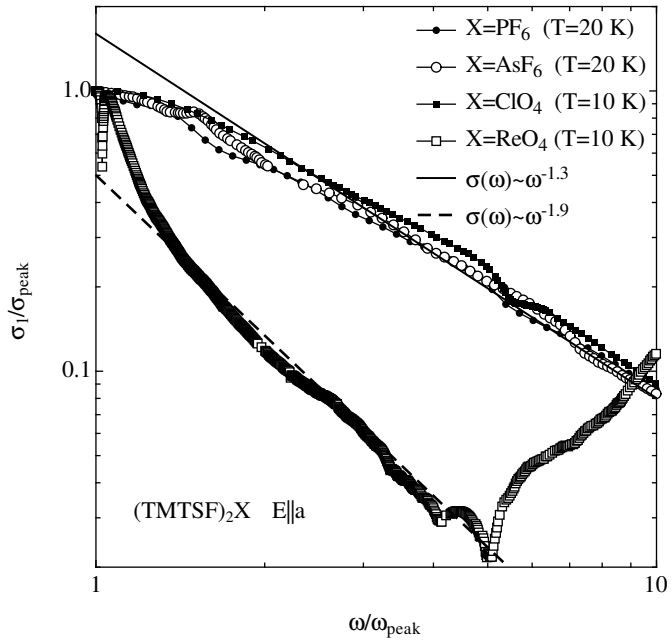

Figure 8: The frequency dependence of the optical conductivity in the spectral range of the finite energy mode (charge gap) in the $(TMTSF)_2X$ salts. The maximum value of $\sigma_1(\omega)$ and the frequency, where the maximum occurs, of the charge gap are represented by σ_{peak} and ω_{peak}, respectively. The solid line is the powerlaw $\sigma_1(\omega)\sim\omega^{-\gamma}$ with γ=1.3 (for X=PF_6, AsF_6 and ClO_4) and γ=1.9 (for X=ReO_4) [35, 37–39].

Fig. 8 shows the frequency dependence of the optical conductivity of the finite energy mode (charge gap) for the $(TMTSF)_2X$ salts in a log-log representation where the optical conductivity and photon energy were normalized by the maximum value σ_{peak} and energy of the gap resonance ω_{peak}, respectively. We clearly observe scaling and a characteristic powerlaw behavior for all the Bechgaard salts. There is a direct relationship to the theoretical expectation. Indeed, at frequencies greater than $t_\perp$, the interchain electron transfer is irrelevant and calculations based on the 1D Hubbard model should be appropriate [21]. As already anticipated above (Fig. 6), the theoretical expectation consists of a powerlaw of the frequency-dependent optical conductivity $\sigma_1(\omega)\sim\omega^{-\gamma}$ for frequencies greater than $t_\perp$ and E_{gap} but less than the on-chain bandwidth $4t_a$. The theory also predicts that the exponent $\gamma = 5 - 4\tilde{n}^2 K_\rho$, K_ρ being the so-called Luttinger liquid parameter and $\tilde{n}$ the degree of commensurability. Our results for X=PF_6, AsF_6 and ClO_4 are consistent with an exponent γ=1.3, indicating a TL liquid (or Luther-Emery (LE) liquid) regime and the predominance

of strong and long-range electronic correlations. This characteristic exponent γ can, in principle, be used to obtain the Luttinger liquid parameter K_ρ, which controls the decay of all correlation functions [21, 35]. In our case and making the assumption that quarter-filled band Umklapp scattering (i.e., $\tilde{n} = 2$) is dominant in the TMTSF family, it then follows γ=5-16K_ρ and $K_\rho \sim 0.23$ [32], which is in reasonable agreement with the photoemission [38] and the transport data, discussed above.

The results regarding the powerlaw behavior are very robust and enable us to discriminate among different regimes and types of correlation. Optical data collected on $(TMTSF)_2ReO_4$ are, in this respect, quite compelling [39]. A Peierls system with dominant CDW correlations, such as $(TMTSF)_2ReO_4$, belongs to the universality class of the LE model [36]. The high frequency tail of the gap feature at 200 meV, below the Peierls transition at 180 K, deserves a particular attention. A fit of the optical conductivity at $\omega > E_{gap}$ (Fig. 8) yields the exponent $\gamma = 1.9$ at 10 K [39]. Theoretically, at photon energies much greater than the energy scale set by the transverse charge transfer integral $t_\perp$ ($\sim$10 meV for the ReO_4 salt), $\gamma \sim 3$ for a rigid lattice with only Umklapp scattering off the single periodic potential, as appropriate for a 1D band insulator. When the coupling to phonons is also included, as in CDW systems, the theory predicts $\gamma \sim 2$. Therefore, our value of γ is in good agreement with the predictions ($\gamma \sim 2$) of the LE scenario. We also note that $\gamma \sim 2$ is considerably different from the γ-values found for other $(TMTSF)_2X$ (X=PF_6, AsF_6 and ClO_4) salts (Fig. 8).

The dimensionality crossover, induced by the increasing $t_\perp (\sim t_b)$ upon pressure or by changing the chemistry (i.e., going from the TMTTF to the TMTSF family), is one of the central issues, when discussing the physics of low dimensional systems. There is a well-established order for $t_\perp$ among the four salts investigated. The $(TMTTF)_2X$ analogs are more anisotropic than the $(TMTSF)_2X$ ones [8]. The values of the transfer integrals along the crystallographic directions (i.e., t_a, t_b and t_c, see Table I) for both groups of salts are in broad agreement with tight-binding model calculations and with the trend indicated by the plasma frequency [35]. It is particularly instructive to compare E_{gap} with t_b. This is shown in Fig. 9 for the four measured Bechgaard salts. To arrive at a scale for t_b, we took the calculated values as averages for the $(TMTSF)_2X$ and $(TMTTF)_2X$ salts, respectively, and assumed that pressure changes t_b in a linear fashion. There is a charge transfer of one

electron to each of the counterions. The positions of the various salts along the horizontal axis of Fig. 9 reflect this choice [38], with pressure values taken from the literature [35, 40].

The solid line in Fig. 9 represents the overall behavior of the correlation gap. Various experiments give slightly different values of the gap. This is probably due to the differences in the curvature of the band, which is scanned differently in the experiments, or due to the difference in spectral response functions involved. The decrease going from the $(TMTTF)_2X$ to the $(TMTSF)_2X$ analogs may represent various factors, such as the decreasing degree of dimerization and the slight increase in the bandwidth along the a axis, as evidenced by the greater value of the plasma frequency measured along the chain direction in the $(TMTSF)_2X$ salts [35]. The dotted line representing $2t_b$ (this is half the bandwidth perpendicular to the chains in the tight-binding approximation) crosses the full line displaying the behaviour of E_{gap} between the salts exhibiting insulating and metallic behaviour, whereas the dotted line representing t_b crosses the solid line between the two metallic salts. Therefore, the experiments strongly suggest that a crossover from a non-conducting (Mott insulator) to a conducting (doped Mott semiconductor) state occurs when the correlation gap exceeds the unrenormalized single particle transfer integral t_b between the chains by a factor A (i.e., $E_{gap} = At_b$), which is on the order of but somewhat greater than 1. This is also evidence of the fact that a confinement-deconfinement crossover by tuning $t_\perp$ is indeed a dimensionality driven insulator-metal transition [37].

Additional evidence of a pronounced qualitative difference between states with $At_b < E_{gap}$ and $At_b > E_{gap}$ is given by plasma frequency studies along the b direction (i.e., perpendicular to the chain). As shown in Ref. 37, there is no well-defined plasma frequency for the insulating state of the TMTTF salts, and we regard this as evidence for the confinement of electrons on individual chains. In fact, the reflectivity has a temperature independent overdamped-like behavior along the b axis. Conversely, the electrons become deconfined as soon as $E_{gap} \sim At_b$ (Fig. 9). Such a deconfinement is manifested by the onset of a sharp plasma edge in the low-temperature reflectivity spectra of the TMTSF salts along the b axis [37]. This finding is not entirely unexpected: a simple argument (the same as one would advance for a band-crossing transition for an uncorrelated band semiconductor) would suggest that to create an electron hole pair with the electron and hole residing on neighbouring chains, an energy comparable to the gap would be required.

Figure 9: The pressure dependence of the (Mott) correlation gap, as established by different experimental methods, and of the transfer integral, perpendicular to the chains, t_b, for the Bechgaard salts [8]. The horizontal scale was derived from results of pressure studies [35, 37, 40].

To summarize, optical data on the prototype linear chain Bechgaard salts reveal the peculiarity of the one-dimensional interacting electron gas response. The unusual spectral features of the Bechgaard salts prove that these materials are certainly not simple anisotropic band metals. Clear deviations from the Fermi liquid behaviour have been identified and several aspects hint to a possible manifestation of a Tomonaga-Luttinger or Luther-Emery liquid in the normal phases. The characteristic energy scale in the optical conductivity data is the Mott-Hubbard gap, of about ~ 25 meV in $(TMTSF)_2PF_6$, with a characteristic Luttinger parameter $K_\rho \sim 0.2$, revealing strong, long-range 1D correlations. Our optical data give evidence of a so-called incipient 2D Fermi liquid scenario in which a low energy 3D Fermi liquid behavior (i.e., represented by the narrow zero energy mode) coexists with the high-energy (1D) TL liquid state (i.e., represented by the powerlaw on the high frequency tail of the charge correlation pseudogap). Our results on Bechgaard salts bear a quite striking similarity to those recently collected in the high temperature superconducting cuprates (HTC) [41]. The scaling and the powerlaw on $\sigma_1(\omega)$ in HTC with

$\gamma = 1.6$ again suggest that the underlying physics in the superconducting cuprates is also intimately related to the 1D character of the electronic transport in the Cu-O chains.

CONCLUSIONS

In conclusion, the studies of the optical and the dc transport properties under pressure of several members of the $(TM)_2X$ series have shown contrasted temperature variations depending on the crystal axis and pressure. They have provided important clues, namely the role of correlations making these quarter-filled 1D conductors Mott insulators, and the interplay between the Mott gap and the transverse coupling allowing a transverse deconfinement of the carriers under pressure and finally to superconductivity under pressure in all of them.

ACKNOWLEDGEMENTS

This communication is based on the original work by P.Auban-Senzier, with the help of C.R. Pasquier, and by V. Vescoli and on the contributions of P. Batail and colleagues at Angers, J.M. Fabre at Montpellier and K. Bechgaard at Copenhagen. This work has also greatly benefited from a close collaboration with T. Giamarchi at Geneva and C. Bourbonnais at Sherbrooke. The authors are very grateful to D. Baeriswyl, P.M. Chaikin, M. Dressel, M. Grioni, G. Gruner, F. Mila and J. Voit for many illuminating discussions. Research at ETH Zurich was supported by the Swiss National Foundation for the Scientific Research.

[1] K. Bechgaard, C. Jacobsen, K. Mortensen, H. Pedersen, and N. Thorup, Solid State Commun. **33**, (1979) 1119.

[2] A. Overhauser, Phys. Rev. Lett. **9**, (1960) 462.

[3] W. M. Lomer, Proc. Phys. Soc. **80**, (1962) 489.

[4] D. Jérome, A. Mazaud, M. Ribault, and K. Bechgaard, J. Phys. (Paris) Lett. **41**, (1980) L95.

[5] S. Parkin, M. Ribault, D. Jérome, and K. Bechgaard, J. Phys. C. **14**, (1981) L.

[6] K. Bechgaard, M. Carneiro, M. Olsen, and F. Rasmussen, Phys. Rev. Lett. **46**, (1981) 852.

[7] D. Jérome, Science **252**, (1991) 1509.

[8] D. Jérome and H. Schulz, Adv. in Physics **31**, (1982) 299.

[9] J. Friedel and D. Jérome, Contemp. Phys. **23**, (1982) 583.

[10] L. Ducasse, A. Abderraba, J. Hoarau, M. Pesquer, B. Gallois, and J. Gaultier, J. Phys. C **39**, (1986) 3805.

[11] K. Behnia, L. Balicas, W. Kang, D. Jérome, Y.F.P. Carretta, C. Berthier, M. Horvatic, P. Ségransan, L. Hubert, and C. Bourbonnais, Phys. Rev. Lett. **74**, (1995) 5272.

[12] P. Auban, D. Jérome, C. Carcel, and J. Fabre, J. Phys. IV France **114**, (2004) 41, and to be published.

[13] K. Heuzé, M. Fourmigué, P. Batail, C. Coulon, R. Clérac, E. Canadell, P. Auban-Senzier, R. Ravy, and D. Jérome, Adv. Mater **15**, (2003) 1251.

[14] E.B. Lopes, H. Alves, E. Ribera, M. Mas-Torrent, P. Auban-Senzier, E. Canadell, R.T. Henriques, M. Almeida, E. Molins, and J. Veciana, Eur. Phys. J. B **29**, (2002) 27.

[15] D. Jaccard, H. Wilhelm, D. Jérome, J. Moser, C. Carcel, and J.M. Fabre, J. Phys. Cond. Mat. **13**, (2001) L-89.

[16] S. Brazovskii and S. Gordyunin, JETP Letters **31**, (1980) 371.

[17] H. J. Schulz, Phys. Rev. Lett. **64**, (1990) 2831.

[18] J. Voit, Rep. Prog. Phys. **58**, (1995) 977.

[19] C. Bourbonnais and D. Jérome: *Advances in Synthetic Metals*, edited by P. Bernier, S. Lefrant and G. Bidan (Elsevier, New York, 1999), p. 206.

[20] J. Solyom, Adv. Phys. **28**, (1979) 201.

[21] T. Giamarchi, Physica **B230-232**, (1997) 975.

[22] C.S. Jacobsen, D. Tanner, and K. Bechgaard, Phys. Rev. Lett. **46**, (1981) 1142 .

[23] J. Moser, M. Gabay, P. Auban-Senzier, D. Jérome, K. Bechgaard, and J. M. Fabre, Eur. Phys. J. B **1**, (1998) 39.

[24] P. Auban, private communication (2005).

[25] N. Mott: *Metal-Insulator Transitions* (Taylor and Francis, London, 1974).

[26] A. Georges, T. Giamarchi, and N. Sandler, Phys. Rev. B. **61**, (2000) 16393.

[27] J. Cooper, Phys. Rev. B **19**, (1979) 2404.

[28] D. Jérome: *Organic Conductors*, ed. J. P. Farges (M. Dekker, New York, 1994), p. 405.

[29] P. Auban-Senzier, D. Jérome, and J. Moser: *Physical Phenomena at High Magnetic Fields-III*, (World Scientific, Singapore, 1999), p. 211.

[30] S. Barisić and S. Brazovskii: *Recent Developments in Condensed Matter Physics*, ed. J. T. Devreese (Plenum Press, New York, 1981), vol. 1, p. 327.

[31] V. J. Emery, R. Bruinsma, and S. Barisić, Phys. Rev. Lett. **48**, (1982) 1039.

[32] A. Schwartz, M. Dressel, G. Grüner, V. Vescoli, L. Degiorgi, and T. Giamarchi, Phys. Rev. B. **58**, (1998) 1261.

[33] S. Biermann, A. Georges, A. Lichtensein, and T. Giamarchi, Phys. Rev. Lett. **87**, (2001)276405.

[34] G. Gruner: *Density Waves in Solids*, (Addison-Wesley, Reading, MA, 1994).

[35] L. Degiorgi: *Strong Interactions in Low Dimensions*, eds. D. Baeriswyl and L. Degiorgi (Vol. 25, Kluwer Academic Publishers, 2004), p. 165.

[36] J. Voit, Eur. Phys. J. B **5**, (1998) 505 and Proceedings of the NATO Advanced Research Workshop on The Physics and Mathematical Physics of the Hubbard Model, San Sebastian, October 3-8, 1993, eds. D. Baeriswyl, D.K. Campbell, J.M.P. Carmelo, F. Guinea, and E. Louis; Plenum Press, New York (1995).

[37] V. Vescoli, L. Degiorgi, W. Henderson, G. Gruner, K.P. Starkey and L.K. Montgomery, Science **281**, (1998) 1181.

[38] V. Vescoli, F. Zwick, W. Henderson, L. Degiorgi, M. Grioni, G. Gruner and L.K. Montgomery, Eur. Phys. J. B **13**, (2000) 503.

[39] F. Zwick, M. Grioni, G. Margaritondo, V. Vescoli, L. Degiorgi, B. Alavi and G. Gruner, Solid State Commun. **113**, (2000) 179.

[40] D. Jérome: *Strongly interacting fermions and high T_C superconductivity*, eds. B. Doucot and J. Zinn-Justin (Elsevier Science, 1995), p. 249.

[41] Y.S. Lee, K. Segawa, Y. Ando and D.N. Basov, Phys. Rev. Lett. **94**, (2005) 137004.